OPTOELECTRONICS AND ADVANCED MATERIALS – RAPID COMMUNICATIONS Vol. 4, No. 9, September 2010, p. 1284 - 1288

Influences of pump-to-Stokes RIN transfer on the single-order silicon Raman lasers

X. LIU[a], X. SANG[a,b*], B. YAN[a], K. WANG[a], C. YU[a], W. DOU[b]
[a]*Key Laboratory of Information Photonics and Optical Communications (Beijing University of Posts and Telecommunications), Ministry of Educations, Post box 72(BUPT), Beijing 100876, China*
[b]*School of Computer Science, National University of Defense Technology, Changsha, Hunan 410073, China*

Pump-to-Stokes relative intensity noise (RIN) transfer in the single-order silicon lasers is numerically investigated. Similar to Raman fiber lasers, RIN transfer makes a great contribution to the output RIN of silicon Raman lasers. Influences of nonlinear losses from two-photon absorption (TPA) and TPA-induced free-carrier absorption (FCA) on the performances of single-order silicon Raman lasers are discussed.

(Received August 8, 2010; accepted September 15, 2010)

Keywords: Silicon Raman Laser, Relative intensity noise (RIN), Nonlinear losses

1. Introduction

In recent years, Silicon-on-insulator (SOI) has attracted much attention for photonic integrated circuits and nonlinear optoelectronic devices because it's highly nonlinear, high-index-contract and transparent to wavelengths above 1.1 μm. Stimulated Raman scatting in silicon is much more stronger than that in glass fiber, which can hurdle the limitation of low emission efficiency because of its indirect bandgap. With this nonlinear effect, light amplification and lasing has been realized in silicon [1-9]. Two main nonlinear losses from two-photon absorption (TPA) and TPA-induced free-carrier absorption (FCA) have significant impacts on optical gain and lasing in silicon [10-13].

Relative intensity noise which is described as small amplitude perturbations on the pump will be transferred to the Stokes during light amplifying and lasing. Recently, we have investigated RIN transfer its influence on noise figure in silicon Raman amplifier [14,15]. Pump-to-stokes RIN transfer is experimentally and numerically showed in Raman fiber lasers [16]. The results from experiment and mathematical model agree well.

Here, pump-to-Signal RIN Transfer and its impact on performance of single-order silicon Raman lasers are presented.

2. Pump-to-Stokes RIN Transfer in sinlg-oder Silicon Raman lasers

In the single-order silicon Raman laser, pump laser at the wavelength λ_p with power $P_0\,(t)$ is coupled from left-hand side of the SOI waveguide. Both end surfaces of the SOI waveguide are coated, and R_l, R_r are reflectivity for stokes λ_s at the left-hand and right-hand sides of the waveguide. Neglecting the influence of phases, only the varying powers of the pump and stokes are considered. The differential equations which characterize the pump, forward-stokes and backward stokes travelling inside the silicon waveguide can be written as follows:

$$\frac{dP_p}{dz}+\frac{1}{v_p}\cdot\frac{dP_p}{dt}=-\alpha_p P_p-\frac{g}{A_{eff}}\frac{\lambda_s}{\lambda_p}(P_s^+ + P_s^-)P_p-\frac{\beta}{A_{eff}}P_p^2-\frac{2\beta}{A_{eff}}(P_s^+ + P_s^-)P_p-\alpha_p^{FCA}P_p \tag{1}$$

$$\frac{dP_s^+}{dz}+\frac{1}{v_s}\cdot\frac{dP_s^+}{dt}=-\alpha_s P_s^+ +\frac{g}{A_{eff}}P_s^+ P_p-\frac{\beta}{A_{eff}}P_s^{+^2}-\frac{2\beta}{A_{eff}}(P_s^- + P_p)P_s^+ -\alpha_s^{FCA}P_s^+ \tag{2}$$

$$\frac{dP_s^-}{dz}-\frac{1}{v_s}\cdot\frac{dP_s^-}{dt}=\alpha_s P_s^- -\frac{g}{A_{eff}}P_s^- P_p+\frac{\beta}{A_{eff}}P_s^{-^2}+\frac{2\beta}{A_{eff}}(P_s^+ + P_p)P_s^- +\alpha_s^{FCA}P_s^- \tag{3}$$

where z is the longitudinal coordinate, P_p 、 P_s^+ 、 P_s^- are the powers of pump, forward-stokes and backward stoke, $v_{p,s}$ are the group velocities experienced by pump and stokes at the wavelengths $\lambda_{p,s}$, $\alpha_{s,p}$ is the linear loss coefficients, g is the Raman gain coefficient which describes the optical powers transferred from pump to Stokes, A_{eff} is the modal effective area, and β is the two-photon absorption coefficient. α_j^{FCA} ($j=p,s$) is given as [15]:

$$\alpha_j^{FCA}=1.45\times10^{-17}\cdot\left(\lambda_j/1550\right)^2 N(z) \tag{4}$$

Where $N(z)$ is the free carrier density. In the case of CW silicon Raman laser, the free carrier density is given by $N(z)=\frac{\tau\beta}{2h\upsilon A_{eff}^2}\left(P_p+P_s^+ + P_s^-\right)^2$. τ is free-carrier life time, $h\nu$ is the photo energy, and h is the planck's constant. The boundary conditions are as follows:

$$P_s^-(L,t) = R_r P_s^+(L,t) \tag{5}$$

$$P_s^+(0,t) = R_l P_s^-(0,t) \tag{6}$$

$$P_p(0,t) = P_0(t) \tag{7}$$

Considering the fluctuations on powers as the noise of the pump laser, the small-signal modulations on pump, forward-stokes and backward-stokes along transmission length z can be given as:

$$P_p(z,t) = \overline{P}_p(z) + p_p(z,t) \tag{8}$$

$$P_s^+(z,t) = \overline{P}_s^+(z) + p_s^+(z,t) \tag{9}$$

$$P_s^-(z,t) = \overline{P}_s^-(z) + p_s^-(z,t) \tag{10}$$

where $p_p(z,t)$ 、 $p_s^+(z,t)$ and $p_s^-(z,t)$ are characterized as the fluctuations for the steady-static powers $\overline{P}_p(z)$, $\overline{P}_s^+(z)$ and $\overline{P}_s^-(z)$. Substituting Eqs.(8)-(10) into (1)-(3) and (5)-(7), steady-static powers satisfy:

$$\frac{d\overline{P}_p}{dz} = -\alpha_p \overline{P}_p - \frac{g}{A_{eff}} \cdot \frac{\lambda_s}{\lambda_p}\left(\overline{P}_s^+ + \overline{P}_s^-\right)\overline{P}_p - \frac{\beta}{A_{eff}}\overline{P}_p^2 - \frac{2\beta}{A_{eff}}\left(\overline{P}_s^+ + \overline{P}_s^-\right)\overline{P}_p - \kappa_p^{FCA}\left(\overline{P}_p + \overline{P}_s^+ + \overline{P}_s^-\right)^2 \cdot \overline{P}_p \tag{12}$$

$$\frac{d\overline{P}_s^+}{dz} = -\alpha_s \overline{P}_s^+ + \frac{g}{A_{eff}} \cdot \overline{P}_s^+ \overline{P}_p - \frac{\beta}{A_{eff}} \overline{P}_s^{+2} - \frac{2\beta}{A_{eff}}\left(\overline{P}_s^- + \overline{P}_p\right)\overline{P}_s^+ - \kappa_s^{FCA}\left(\overline{P}_p + \overline{P}_s^+ + \overline{P}_s^-\right)^2 \cdot \overline{P}_s^+ \tag{13}$$

$$\frac{d\overline{P}_s^-}{dz} = \alpha_s \overline{P}_s^- - \frac{g}{A_{eff}} \cdot \overline{P}_s^- \overline{P}_p + \frac{\beta}{A_{eff}} \overline{P}_s^{-2} + \frac{2\beta}{A_{eff}}\left(\overline{P}_s^+ + \overline{P}_p\right)\overline{P}_s^- + \kappa_s^{FCA}\left(\overline{P}_p + \overline{P}_s^+ + \overline{P}_s^-\right)^2 \cdot \overline{P}_s^- \tag{14}$$

$$\overline{P}_s^-(L) = R_r \overline{P}_s^+(L) \tag{15}$$

$$\overline{P}_s^+(0) = R_l \overline{P}_s^-(0) \tag{16}$$

$$\overline{P}_p^+(0) = \overline{P}_0 \tag{17}$$

The small-signal power partial differential equations can be derived as:

$$\frac{dp_p}{dz} + \frac{1}{v_p}\cdot\frac{dp_p}{dt} = -\alpha_p p_p - \frac{g}{A_{eff}} \cdot \frac{\lambda_s}{\lambda_p}\left(\overline{P}_s^+ + \overline{P}_s^-\right)p_p - \frac{g}{A_{eff}} \cdot \frac{\lambda_s}{\lambda_p}\left(p_s^+ + p_s^-\right)\overline{P}_p - \frac{2\beta}{A_{eff}} \cdot \overline{P}_p p_p - \frac{2\beta}{A_{eff}} \cdot \left(\overline{P}_s^+ + \overline{P}_s^-\right) \cdot p_p - \frac{2\beta}{A_{eff}} \cdot \left(p_s^+ + p_s^-\right) \cdot \overline{P}_p - \kappa_p^{FCA} \cdot \Delta_1 \tag{18}$$

$$\frac{dp_s^+}{dz} + \frac{1}{v_s}\cdot\frac{dp_s^+}{dt} = -\alpha_s p_s^+ + \frac{g}{A_{eff}}\overline{P}_s^+ p_p + \frac{g}{A_{eff}}\overline{P}_p p_s^+ - \frac{2\beta}{A_{eff}}\overline{P}_s^+ p_s^+ - \frac{2\beta}{A_{eff}} \cdot \left(\overline{P}_s^- + \overline{P}_p\right) \cdot p_s^+ - \frac{2\beta}{A_{eff}} \cdot \left(p_s^- + p_p\right) \cdot \overline{P}_s^+ - \kappa_s^{FCA} \cdot \Delta_2 \tag{19}$$

$$\frac{dp_s^-}{dz} - \frac{1}{v_s}\cdot\frac{dp_s^-}{dt} = \alpha_s p_s^- - \frac{g}{A_{eff}}\overline{P}_s^- p_p - \frac{g}{A_{eff}}\overline{P}_p p_s^- + \frac{2\beta}{A_{eff}}\overline{P}_s^- p_s^- + \frac{2\beta}{A_{eff}} \cdot \left(\overline{P}_s^+ + \overline{P}_p\right) \cdot p_s^- + \frac{2\beta}{A_{eff}} \cdot \left(p_s^+ + p_p\right) \cdot \overline{P}_s^- + \kappa_s^{FCA} \cdot \Delta_3 \tag{20}$$

$$p_s^-(L,t) = R_r p_s^+(L,t) \tag{21}$$

$$p_s^+(0,t) = R_l p_s^-(0,t) \tag{22}$$

$$p_p(0,t) = p_0(t) \tag{23}$$

where

$$\Delta_1 = 3\overline{P}_p^{\,2} p_p + \overline{P}_s^{+2} p_p + \overline{P}_s^{-2} p_p + 4\overline{P}_p \overline{P}_s^+ p_p + 4\overline{P}_p \overline{P}_s^- p_p + 2\overline{P}_s^+ \overline{P}_s^- p_p + 2\overline{P}_p^{\,2} p_s^+ + 2\overline{P}_p^{\,2} p_s^- + 2\overline{P}_p \overline{P}_s^+ p_s^+ + 2\overline{P}_p \overline{P}_s^+ p_s^- + 2\overline{P}_p \overline{P}_s^- p_s^+ + 2\overline{P}_p \overline{P}_s^- p_s^-$$

$$\Delta_2 = \overline{P}_p^{\,2} p_s^+ + 3\overline{P}_s^{+2} p_s^+ + \overline{P}_s^{-2} p_s^+ + 4\overline{P}_p \overline{P}_s^+ p_s^+ + 2\overline{P}_p \overline{P}_s^- p_s^+ + 4\overline{P}_s^+ \overline{P}_s^- p_s^+ + 2\overline{P}_p \overline{P}_s^+ p_p + 2\overline{P}_p \overline{P}_s^+ p_s^- + 2\overline{P}_s^{+2} p_p + 2\overline{P}_s^{+2} p_s^- + 2\overline{P}_s^+ \overline{P}_s^- p_p + 2\overline{P}_s^+ \overline{P}_s^- p_s^-$$

$$\Delta_3 = \overline{P}_p^{\,2} p_s^- + \overline{P}_s^{+2} p_s^- + 3\overline{P}_s^{-2} p_s^- + 2\overline{P}_p \overline{P}_s^+ p_s^- + 4\overline{P}_p \overline{P}_s^- p_s^- + 4\overline{P}_s^+ \overline{P}_s^- p_s^- + 2\overline{P}_p \overline{P}_s^- p_p + 2\overline{P}_p \overline{P}_s^- p_s^+ + 2\overline{P}_s^+ \overline{P}_s^- p_p + 2\overline{P}_s^+ \overline{P}_s^- p_s^+ + 2\overline{P}_s^{-2} p_p + 2\overline{P}_s^{-2} p_s^+$$

$$\kappa_{p,s}^{FCA} = \alpha_{p.s}^{FCA} / \left(P_p + P_s^+ + P_s^-\right)^2$$

Assuming that the fluctuations are much smaller than steady-state values, the Fourier transform are carried in the above equations [17]. The small-signal power differential equations and boundary conditions are given as follows:

$$\frac{d\tilde{p}_p}{dz} = -\alpha_p \tilde{p}_p - \frac{j\omega}{v_p}\cdot\tilde{p}_p - \frac{g}{A_{eff}} \cdot \frac{\lambda_s}{\lambda_p}\left(\overline{P}_s^+ + \overline{P}_s^-\right)\tilde{p}_p - \frac{g}{A_{eff}} \cdot \frac{\lambda_s}{\lambda_p}\left(\tilde{p}_s^+ + \tilde{p}_s^-\right)\overline{P}_p - \frac{2\beta}{A_{eff}} \cdot \overline{P}_p \tilde{p}_p - \frac{2\beta}{A_{eff}} \cdot \left(\overline{P}_s^+ + \overline{P}_s^-\right) \cdot \tilde{p}_p - \frac{2\beta}{A_{eff}} \cdot \left(\tilde{p}_s^+ + \tilde{p}_s^-\right) \cdot \overline{P}_p - \kappa_p^{FCA} \cdot \Delta_1^* \tag{24}$$

$$\frac{d\tilde{p}_s^+}{dz} = -\alpha_s \tilde{p}_s^+ - \frac{j\omega}{v_s}\cdot\tilde{p}_s^+ + \frac{g}{A_{eff}}\overline{P}_s^+ \tilde{p}_p + \frac{g}{A_{eff}}\overline{P}_p \tilde{p}_s^+ - \frac{2\beta}{A_{eff}}\overline{P}_s^+ \tilde{p}_s^+ - \frac{2\beta}{A_{eff}} \cdot \left(\overline{P}_s^- + \overline{P}_p\right) \cdot \tilde{p}_s^+ - \frac{2\beta}{A_{eff}} \cdot \left(\tilde{p}_s^- + \tilde{p}_p\right) \cdot \overline{P}_s^+ - \kappa_s^{FCA} \cdot \Delta_2^* \tag{25}$$

$$\frac{d\tilde{p}_s^-}{dz} = \alpha_s \tilde{p}_s^- + \frac{j\omega}{v_s}\cdot\tilde{p}_s^- - \frac{g}{A_{eff}}\overline{P}_s^- \tilde{p}_p - \frac{g}{A_{eff}}\overline{P}_p \tilde{p}_s^- + \frac{2\beta}{A_{eff}}\overline{P}_s^- \tilde{p}_s^- + \frac{2\beta}{A_{eff}} \cdot \left(\overline{P}_s^+ + \overline{P}_p\right) \cdot \tilde{p}_s^- + \frac{2\beta}{A_{eff}} \cdot \left(\tilde{p}_s^+ + \tilde{p}_p\right) \cdot \overline{P}_s^- + \kappa_s^{FCA} \cdot \Delta_3^* \tag{26}$$

$$\tilde{p}_s^-(L,\omega) = R_r \tilde{p}_s^+(L,\omega) \tag{27}$$

$$\tilde{p}_s^+(0,\omega) = R_l \tilde{p}_s^-(0,\omega) \tag{28}$$

$$\tilde{p}_p(0,\omega) = \tilde{p}_0(\omega) \tag{29}$$

where

$$\Delta_1^* = 3\bar{P}_p^2\tilde{p}_p + \bar{P}_s^{+2}\tilde{p}_p + \bar{P}_s^{-2}\tilde{p}_p + 4\bar{P}_p\bar{P}_s^+\tilde{p}_p + 4\bar{P}_p\bar{P}_s^-\tilde{p}_p + 2\bar{P}_s^+\bar{P}_s^-\tilde{p}_p + 2\bar{P}_p^2\tilde{p}_s^+ + 2\bar{P}_p^2\tilde{p}_s^- + 2\bar{P}_p\bar{P}_s^+\tilde{p}_s^+ + 2\bar{P}_p\bar{P}_s^+\tilde{p}_s^- + 2\bar{P}_p\bar{P}_s^-\tilde{p}_s^+ + 2\bar{P}_p\bar{P}_s^-\tilde{p}_s^-$$

$$\Delta_2^* = \bar{P}_p^2\tilde{p}_s^+ + 3\bar{P}_s^{+2}\tilde{p}_s^+ + \bar{P}_s^{-2}\tilde{p}_s^+ + 4\bar{P}_p\bar{P}_s^+\tilde{p}_s^+ + 2\bar{P}_p\bar{P}_s^-\tilde{p}_s^+ + 4\bar{P}_s^+\bar{P}_s^-\tilde{p}_s^+ + 2\bar{P}_p\bar{P}_s^+\tilde{p}_p + 2\bar{P}_p\bar{P}_s^+\tilde{p}_s^- + 2\bar{P}_s^{+2}\tilde{p}_p + 2\bar{P}_s^{+2}\tilde{p}_s^- + 2\bar{P}_s^+\bar{P}_s^-\tilde{p}_p + 2\bar{P}_s^+\bar{P}_s^-\tilde{p}_s^-$$

$$\Delta_3^* = \bar{P}_p^2\tilde{p}_s^- + \bar{P}_s^{+2}\tilde{p}_s^- + 3\bar{P}_s^{-2}\tilde{p}_s^- + 2\bar{P}_p\bar{P}_s^+\tilde{p}_s^- + 4\bar{P}_p\bar{P}_s^-\tilde{p}_s^- + 4\bar{P}_s^+\bar{P}_s^-\tilde{p}_s^- + 2\bar{P}_p\bar{P}_s^-\tilde{p}_p + 2\bar{P}_p\bar{P}_s^-\tilde{p}_s^+ + 2\bar{P}_s^+\bar{P}_s^-\tilde{p}_p + 2\bar{P}_s^+\bar{P}_s^-\tilde{p}_s^+ + 2\bar{P}_s^{-2}\tilde{p}_p + 2\bar{P}_s^{-2}\tilde{p}_s^+$$

Hence, the RIN transfer function can be achieved as follows

$$T_{RIN}(\omega) = \left[\frac{\left|\tilde{p}_{out}(\omega)\right| / \bar{P}_{out}}{\left|\tilde{p}_0(\omega)\right| / \bar{P}_0}\right]^2 \qquad (30)$$

where

$$\tilde{p}_{out}(\omega) = \tilde{p}_s^+(L,\omega) - \tilde{p}_s^-(L,\omega),$$
$$\bar{P}_{out} = \bar{P}_s^+(L) - \bar{P}_s^-(L)$$

3. Simulation results

3.1 Pump-to-Signal RIN Transfer in silicon Raman laser

The RIN transfer ($10\log T_{RIN}(\omega)$) can be numerically calculated in the silicon Raman lasers by Eqs.(18)-(30), where the waveguide length L is 4.8 cm, linear loss coefficient $\alpha_p = \alpha_s = 1dB/cm$, Raman gain coefficient $g = 20cm/GW$, two photon absorption TPA coefficient $\beta = 0.7cm/GW$, and the effective modal area is $A_{eff} = 5um^2$ [13]. The pump wavelength is $\lambda_p = 1540nm$. Due to Raman frequency shift of 15.6 THz from pump wavelength, stokes wavelength is $\lambda_s = 1675nm$ [3].The reflectivity of end-faces for stokes are $R_l = 90\%$, $R_r = 40\%$. By setting $v_p = c/n$, where n =3.45is the average index of silicon, c is the speed of light in vacuum and $D = -910\,ps/(nm\cdot km)$, we can get v_s through $v_s = 1/\left[(\lambda_s - \lambda_p)D + 1/v_p\right]$. The longitudinal cavity resonance at integer multiples of the inverse cavity round-time is described as $f = c/2nl \approx 1\,GHz$. Fig. 1 shows the relative intensity RIN transfer from pump to Stokes in the case of different pump powers of $2w, 3w, 4w$ with free carrier lifetime $\tau = 1ns$, TPA coefficient $\beta = 0.7cm/GW$. The frequency range of transverse coordinate is from 10^6 to $10^{10}Hz$. The value of RIN transfer observed decreases obviously along with increasing pump powers. At lower frequency, RIN transfer keeps a fixed value. High-frequency RIN transfer begin to show intense oscillation at about $10^9 Hz$. This is several orders higher than that in Raman fiber laser (about $10^4 Hz$).

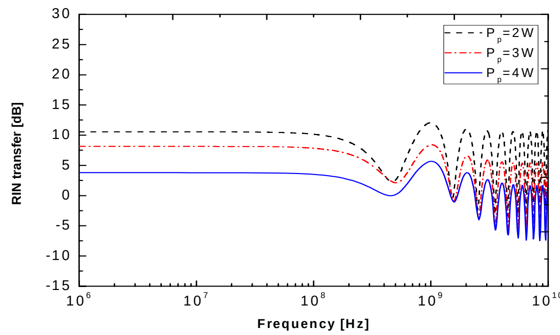

Fig. 1. RIN transfer in silicon Raman lasers under different pump powers with frequency range from 10^6 to 10^{10} Hz. Modal parameters: $L = 4.8cm$, $\alpha_p = \alpha_s = 1dB/cm$, $g = 20cm/GW$, $\beta = 0.7cm/GW$, $\tau = 1ns$, $\lambda_p = 1540nm$, $\lambda_s = 1675nm$.

Fig. 2 shows the RIN transfer under different free carrier lifetime values $0.5ns$, $1ns$, $2ns$ when the pump power is $3\,W$. It is clear that RIN transfer decreases with the increasing τ value which determines Raman gain. RIN transfer in silicon Raman laser has a significant impact on the output RIN in SOI Raman laser and it has a relationship with the value of free carrier lifetime τ.

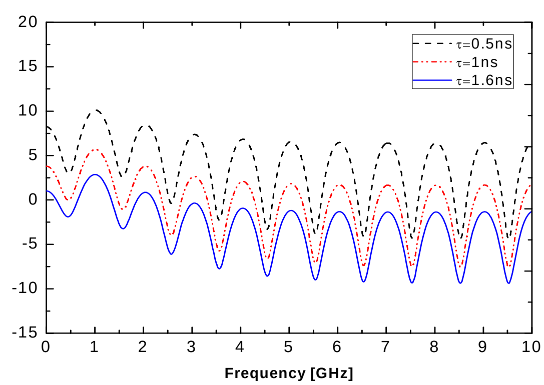

Fig. 2. RIN transfer in silicon Raman lasers under different free carrier lifetime with frequency range from 0 to 10 GHz. Modal parameters $L = 4.8cm$, $\alpha_p = \alpha_s = 1dB/cm$, $g = 20cm/GW$, $\beta = 0.7cm/GW$, $P_p = 3W$, $\lambda_p = 1540nm$, $\lambda_s = 1675nm$.

3.2 RIN Transfer's impact on performance of silicon Raman lasers

To evaluate the influence of RIN transfer on silicon Raman lasers, the longitudinal distribution of the pump, forward stokes and backward tokes inside the silicon waveguide is shown in Fig. 3 (a) and (b). The pump is modulated by the sinusoidal function as $P_p(t) = 4.5 + \cos(2\pi ft)/2$. The longitudinal cavity resonance here is $f = c/2nl \approx 0.43GHz$. We can see that in Fig. 3(a) the modulation of the forward Stokes and backward Stokes are small Compared to results of Fig. 3(a) operating in off-resonance mode, Fig. 3(b) shows the resonance case. Three light have the resonance peaks at the same time in the cavity. The collision of Stokes in Fig. 3(b) are much more intense than that in Fig. 3(a) due to the resonant conditions.

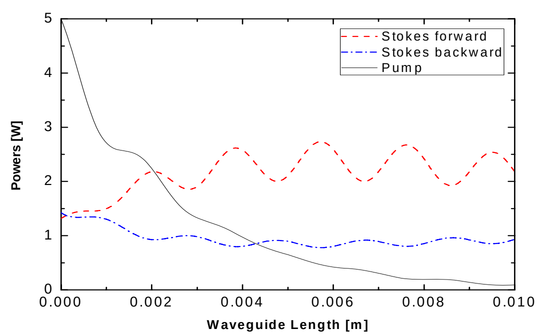

Fig. 3(a). Longitudinal distribution of the pump, forward stokes and backward stokes along the silicon waveguide in the case of $10.5f$. $P_p = 4.5 + \cos(2\pi ft)/2$ under the sinusoidal modulation, $L = 1cm$ $\alpha_p = \alpha_s = 1dB/cm$, $g = 20cm/GW$, $\beta = 0.7cm/GW$, $\tau = 1ns$, $\lambda_p = 1540nm$, $\lambda_s = 1675nm$.

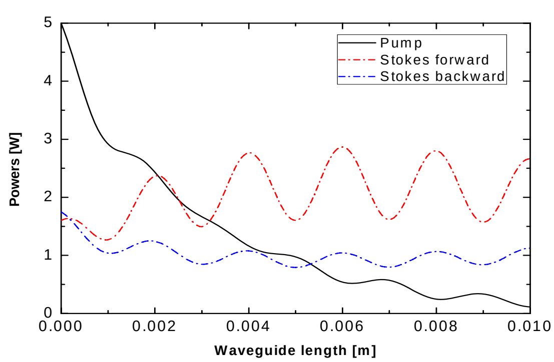

Fig. 3 (b). Longitudinal distribution of the pump, forward stokes and backward stokes along the silicon waveguide in the case of $10f$. $P_p = 4.5 + \cos(2\pi ft)/2$ under the sinusoidal modulation, $L = 1cm$ $\alpha_p = \alpha_s = 1dB/cm$, $g = 20cm/GW$, $\beta = 0.7cm/GW$, $\tau = 1ns$, $\lambda_p = 1540nm$, $\lambda_s = 1675nm$.

Fig. 4 and Fig. 5 reveal the effect of TPA and FCA to the longitudinal distribution of the pump and forward stokes. We can see that FCA has a much more dramatic effect than TPA. Forward Stokes and pump decrease as τ increases. If the value of free carrier lifetime τ is big enough, there will be no output laser at the right-hand side of the cavity.

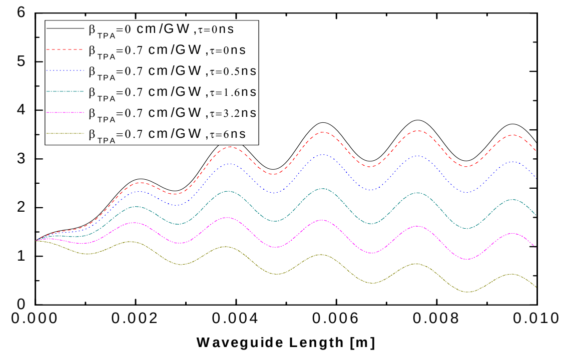

Fig. 4. Longitudinal distribution of forward stokes along the silicon waveguide in the case of $10.5f$ under different values of β and τ. $L = 1cm$, $\alpha_p = \alpha_s = 1dB/cm$, $g = 20cm/GW$, $\lambda_p = 1540nm$, $\lambda_s = 1675nm$.

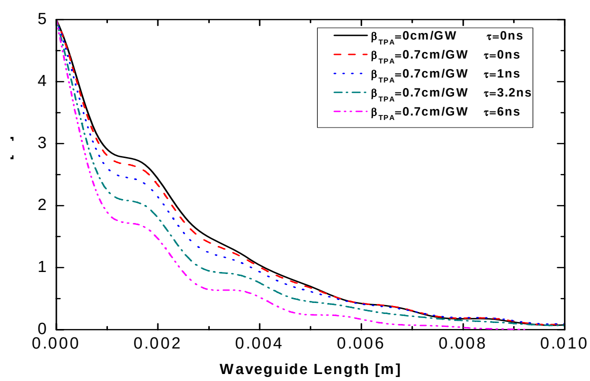

Fig. 5. Longitudinal distribution of the pump along the silicon waveguide in the case of $10.5f$ under different values of β and τ. $L = 1cm$, $\alpha_p = \alpha_s = 1dB/cm$, $g = 20cm/GW$, $\lambda_p = 1540nm$, $\lambda_s = 1675nm$.

4. Conclusion

We show that RIN transfer will have a great important influence on the performances of single-order silicon Raman lasers. Due to inefficient "walk-off" between pump and Stokes, the power fluctuations resided on the pump will be transferred to the output laser. By analyzing the longitudinal distribution of pump and Stokes in silicon Raman lasers, we show that RIN transfer has a much more intense operation on forward and backward Stokes in the resonance mode than that in off-resonance case. RIN transfer is important for applications of silicon Raman lasers.

Acknowledgments

This work is partly supported by the National Key Basic Research Special Foundation (2010CB327601), the Key Project of Chinese Ministry of Education (No.109015), the National Science Foundation of China (60807022), and the China Postdoctoral Science Foundation (20100471788).

References

[1] T. K. Liang, H. K. Tsang, Appl. Phys. Lett., **85**, 3343 (2004).
[2] O. Boyraz, B. Jalali, Electron. Expr., **1**, 429 (2004).
[3] O. Boyraz, B. Jalali, Opt.Express, **12**, 5269 (2004).
[4] O. Boyraz, B. Jalali, Opt.Express, **13**(3), 796 (2005).
[5] H. Rong, R. Jones, A. Liu et al., Nature, **433**, 725 (2005).
[6] H. Rong, et al. Nature **433**, 292 (2005).
[7] Haisheng Rong, Ying-Hao Kuo, Shengbo Xu, Ansheng Liu, Richard Jones, Mario Paniccia, Opt. Express, **14**(15), 6705 (2006).
[8] X. Sang, E.-K. Tien, N. S. Yuksek, F. Qian, Q. Song, O. Boyraz, IEEE Photon. Technol. Lett. **20**(13), 1184 (2008).
[9]A. Liu, et al. J. Lightwave Tech. **24,** 1440 (2006).
[10] R. Claps, V. Raghunathan, D. Dimitropoulos, B. Jalali, Opt. Express **12**(12), 2774 (2004).
[11] T. K. Liang, H. K. Tsang, Appl. Phys. Lett. **84**(15), 2745 (2004).
[12] H. Rong, et al. Proc of SPIE 5931, 59310R 1-9 (2006).
[13]Michael Krause, Hagen Renner, Ernst Brinkmeyer, Opt. Express, **12**(23), 5703 (2004).
[14] X. Liu, X. Sang, X. Liu, B. Yan, K. Wang, C. Yu, Optoelectron. Adv. Mater. Rapid Comm. **4**, 929 (2010).
[15] X. Sang, D. Dimitropoulos, B. Jalali, O. Boyraz, IEEE Photon. Technol Lett, **20**(24), 1041 (2008).
[16] Michael Krause, Sven Cierullies, Hagen Renner, Ernst Brinkmeyer, Optics Communications, **260**, 656 (2006).
[17] S. A. Babin, D. V. Churkin, S. I. Kablukov, E. V. Podivilov, O. I. Medvedkov, A. A. Fotiadi, IEEE Photon. Technol. Lett. **17**(12), 2553 (2005).

*Corresponding author: xzsang@bupt.edu.cn